

# Algorithm development for retrieval of biophysical parameter from ISRO's future GISAT Mission

*Rahul Nigam<sup>1\*</sup>, Bimal K. Bhattacharya<sup>1</sup> and R.P. Singh<sup>2</sup>*

<sup>1</sup>Agriculture and Land Eco-system Division (BPSG)

<sup>2</sup> Land Hydrology Division (GHCAG)

Earth, Ocean, Atmosphere, Planetary Sciences and Applications Area  
Space Applications Centre (ISRO) Ahmedabad – 380 015

## ABSTRACT

The booming development of land-surface ecosystems modeling and environmental monitoring systems has resulted in an urgent demand for high-quality, long-term consistent biophysical parameters such leaf area index (LAI). Canopy radiative transfer (CRT) based methodology has been developed to retrieve agricultural LAI at spatial scale at regular temporal interval. *ProSail* CRT model was customized for future ISRO's GISAT (Geo-stationary Imaging Satellite) MX-VNIR spectral bands. MX-VNIR cover spectral range from 450-520 (B1), 520-590 (B2), 620-680 (B3), 770-860 (B4), 710-740 (B5) to 845-875 (B6) nm. The model was calibrated using two years of measured ground data over six ground sites representing diverse cropping pattern and representing different agro-climatic zones in India. The model was further customized for GISAT MX-VNIR bands using AVIRIS-NG data to evaluate its performance at spatial scale. CRT model inverted to retrieve LAI over Kota region to evaluate performance of developed methodology and respective MX-VNIR bands using AVIRIS-NG data. Retrieved LAI showed RMSE of 0.48 for B2B3B4 bands combinations with measurement. The RMSE increased for B2B3B6 and B2B3B4B5 bands combinations. The bands combination of B2B3B4 was found to be best for retrieval of LAI. The developed methodology will be used to generate operational agricultural LAI at regular interval using GISAT MX-VNIR data.

*Key words: GISAT, AVIRIS, LAI, Radiative transfer model*

*\* Corresponding author: e mail- rahulnigam@sac.isro.gov.in*

## 1. Introduction

Leaf area index (LAI), defined as one half of the total leaf surface area per unit horizontal ground surface area (Chen & Black, 1992), measures the amount of leaf material in an ecosystem, which imposes significant controls on photosynthesis, respiration, rain interception, and other processes (Running, 2000). Consequently, LAI is a key variable that links vegetation to the terrestrial ecosystem productivity model (Marie et al., 2011), energy, and mass exchange between the land surface and the atmosphere (Sellers et al., 1997). LAI is one of the primary measures of biophysical characteristic of vegetation used in process-based models to characterize plant canopies through remote sensing (Bonan, 1993). LAI estimates are used for two basic purposes: (1) as an ecophysiological measure of the photosynthetic and transpirational surface within a

canopy, and (2) as a remote sensing measure of the leaf reflective surface within a canopy. Currently, two approaches are widely used to estimate LAI from satellite data (Propastin and Erasim, 2010). The first uses empirical or semi-empirical statistical relationships between LAI and spectral vegetation indices (Liu et al., 2014). These indices are designed as a combination of surface reflectance to maximize information about canopy characteristics and minimize interference factors from the atmosphere and soil. The second approach is the inversion of a radiative-transfer model that simulates surface reflectance from canopy structure parameters (e.g., LAI), soil, leaf bio-physical-optical properties, and view illumination geometry (Xiao, et al, 2013). Moreover, simulated lookup tables (LUTs) (Shabanov et al., 2005) and trained neural networks (NNs) (Bacour et al, 2006; Walthalla et al., 2004) are commonly used to simplify the process of deriving radiative-transfer models and to improve the efficiency of inversion. In practice, LAI retrieval from remotely sensed data faces two major difficulties: (1) vegetation indices approach a saturation level asymptotically when LAI exceeds 2 to 5, depending on the type of vegetation index; (2) there is no unique relationship between LAI but rather a family of relationships, each a function of canopy characteristics. To address these issues, a few studies have been carried out to assess and compare various vegetation indices in terms of their stability and their prediction power of LAI in various part of world (Baret and Guyot, 1991, Broge and Leblanc, 2000; Tian & Chen, 2010). The crop-specific sensitivity of spectral reflectance relationships to canopy geometry (e.g. leaf angle distribution and clumping) and leaf properties (e.g. dry matter and mesophyll structure) and the site-specific sensitivity to atmospheric and background influences must be properly modeled in order to simulate canopy spectral signature through physical canopy radiative transfer models. At present in India no operational mechanism is available to retrieve LAI as a product from Indian satellite. To address present demand as well as to get operational product from Indian satellite a study was carried out to demonstrate a methodology to retrieve LAI from ISRO's future mission such as GISAT. To address aforementioned limitation, the objectives of this present study were (i) to develop an algorithm to retrieve LAI from ISRO's future GISAT mission, (ii) to test the develop algorithm using AVIRIS data and (iii) validation of retrieved LAI with *in situ* data.

## **2. Study area**

In the present study Kota (Rajasthan) has been selected to test the developed methodology for LAI retrieval as this site was covered in airborne AVIRIS mission. Kota site represents a homogeneous crop area and dominated with wheat crop, mustard and chickpea crops and lies

under Central Plateau & Hill Region (CPHR). Airborne AVIRIS-NG campaign over Kota was conducted on 5<sup>th</sup> February 2016. The site details are shown in Figure 1.

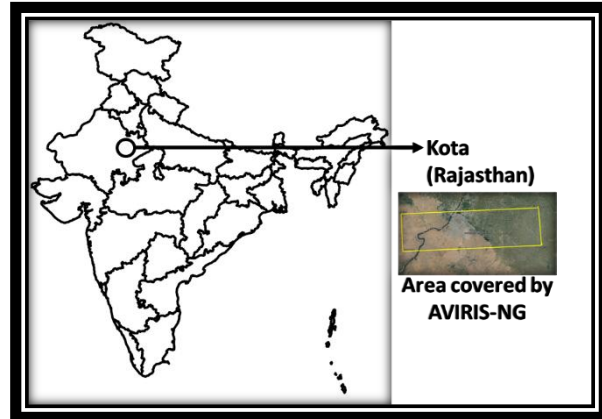


Figure 1. Study area for *in situ* and airborne AVIRIS-NG observations

## 2.1 GISAT specifications

The proposed specification for GISAT is given in Table 1 (Anonymous, 2014).

Table 1. Proposed specification for GISAT Mission

Sensor	SNR / NE $\delta$ T	IGFOV (m)	Range (nm)	Bands (nm)
MX-VNIR	>200	42	450-860	B1: 450-520, B2: 520-590 B3: 620-680 B4: 770-860 B5: 710-860 B6: 845-875
HyS-VNIR	>400	158	357-1100	$\Delta\lambda \approx 4$ nm
HyS-SWIR	>400	256	900-2500	$\Delta\lambda \approx 7$ nm
MX-LWIR	NE $\delta$ T < 0.15K	1200	700-1350	B1: 710-760, B2: 830-870, B3: 940-980,

---

B4: 1030-  
1130,  
B5: 1150-  
1250,  
B6: 1300-  
1350

---

To retrieve regular LAI over agricultural area MX-VNIR bands are planned to be used due to its high temporal resolution.

### 3. Data used

#### 3.1 *In situ* measurements

The following crop parameters were measured during agricultural season during field measurement campaign.

- 
- |   |                         |
|---|-------------------------|
| 1. Phenological stage of the crop   | 7. Leaf size/dimensions |
| 2. Leaf area index  | 8. Crop height (cm)     |
| 3. Mean tilt angle  | 9. Chlorophyll index    |
| 4. Leaf chlorophyll content ( $\mu\text{g cm}^{-2}$ of fresh leaf weight) | 10. Soil reflectance    |
| 5. Leaf equivalent water thickness (cm)                                   | 11. Crop reflectance    |
| 6. Leaf dry matter content ( $\text{g cm}^{-2}$ )                         | 12. Crop photographs    |
- 

#### 3.2 Airborne data

In this study Airborne Visible-Infrared Imaging Spectrometer Next Generation (AVIRIS-NG) hyperspectral data along with *in situ* data during the flight time has been used. AVIRIS-NG has 425 spectral bands between 380 nm to 2500 nm. The spatial resolution is varying from 4 m to 8 m as per the altitude of the flight. The AVIRIS-NG instrument uses most advanced state-of-the-art detector array and grating for dispersion of light. In this study atmospherically corrected L-2

data over Kota region was used. The AVIRIS-NG provides data from 375 nm to 2500 nm. Hence all six MX-VNIR bands were convoluted from AVIRIS-NG data for the present study. This dataset act as surrogate data to evaluate the performance of all MX-VNIR bands for retrieval of LAI.

## 4. Methodology

### 4.1 Canopy radiative transfer (CRT) model

One dimensional (1-D) canopy radiative transfer (CRT) simulation model, PROSAIL, is the combined form of PROSPECT and SAIL. The PROSPECT simulates reflectances at leaf level and SAIL (Scattering by Arbitrary Inclined Leaves) addresses the directionality. The PROSPECT pioneered the simulation of directional-hemispherical reflectances and transmittances (Schaepman-Strub et al., 2006) of various green monocotyledonous and dicotyledonous species, as well as senescent leaves (Verhoef and Bach, 2003), over the vegetation sensitive solar spectrum from 400 nm to 2500 nm (Jacquemoud and Baret, 1990). It is primarily based on the representation of the leaf as one or several absorbing thin plates with rough surfaces giving rise to isotropic scattering (Allen et al., 1969). In PROSPECT inputs are leaf structure parameter ( $N$ ), chlorophyll (a + b) content ( $C_{ab}$ ), leaf equivalent water thickness ( $C_w$ ), leaf dry matter content ( $C_m$ ) and leaf size to crop height ( $S_i$ ). The absorption of light by photosynthetic pigments which is predominant in the visible (VIS) spectrum assumed to be entirely caused by chlorophylls, leaf water content ( $C_w$ ) and dry matter. These model input variables define the optical properties of leaf using leaf mesophyll and biochemical information. Since leaf reflectance, leaf transmittance, and soil reflectance are three wavelength-dependent input variables of SAIL, the implementation of this model to retrieve biophysical variables from canopy reflectance spectra at given solar and viewing angles in a defined relative azimuthal plane requires at least three times as many variables as wavelengths. As a consequence, the inversion of SAIL is generally impracticable unless several viewing angles are available. To reduce the dimensionality of the inverse problem and to assess the canopy biochemistry, SAIL was coupled with PROSPECT to derive PROSAIL (Baret et al., 1992). SAIL is one of the earliest canopy reflectance models (Verhoef, 1984) and was coupled with PROSPECT early in the 1990s to derive PROSAIL (Jacquemoud et al., 2009). The SAIL simulates canopy reflectances as a function of leaf area index (LAI), leaf inclination angle (LIA), hot spot parameter (SL), horizontal visibility ( $vis$ ), sun zenith angle ( $\theta_s$ ), view zenith angle ( $\theta_v$ ), relative azimuth angle ( $\phi_{sv}$ ) and soil albedo ( $\rho_s$ ). The coupling simply consists in passing the output leaf reflectance and transmittance of the PROSPECT model into the SAIL model to simulate the whole spectro-directional canopy reflectance field. The soil spectral or directional reflectance is also required as input to SAIL.

## 4.2 Forward simulation

The CRT model was run in forward mode to generate reflectance for different leaf area index (LAI) values from 1 to 4 with an interval of 0.5 with no change in other input parameters. The generated simulated reflectance showed unique spectral signature for 400-2500 nm wavelength for each LAI value as shown in Figure 2. The mean ( $\mu$ ) and standard deviation ( $\sigma$ ) also computed for all wavelength. The standard deviation was for blue spectral band vary from 0.0005 to 0.001, green 0.001 to 0.04, red 0.05 to 0.35, red edge 0.35 to 0.36 and NIR 0.35 to 0.24 further gradually decreases in SWIR 1 and SWIR 2 spectral band. The maximum deviation was observed in red edge, red and NIR spectral band region. In all these spectral bands change in leaf area index alters the absorption and transmission value with varying magnitude. The blue region does not show much change with varying LAI due to its sensitivity to chlorophyll content only. This region remains less photosynthesis efficient than red band as after excitation with blue photon, the electron always decays extremely rapidly by heat release to a lower energy level that red band produces without heat loss. Green and red bands showed more sensitivity towards LAI. In plant their absorption is not only sensitive to chlorophyll content but also show to other photosynthetically active pigments. Rest of the bands showed high sensitivity for LAI value as their penetration within canopy as well as reflection due to total internal refraction were more and well correlated with canopy vigour.

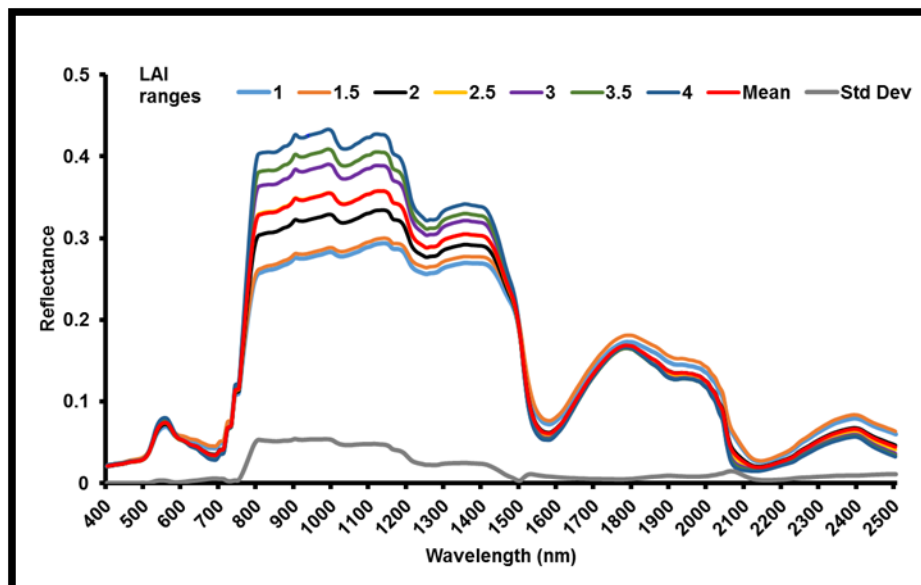


Figure 2. Simulated reflectance with varying LAI

### **4.3 Model performance over GISAT MX-VNIR spectral bands**

Spectral response function of all bands were integrated into model to simulate reflectance for GISAT six MX-VNIR (B1: 450-520, B2: 520-590, B3: 620-680, B4: 770-860, B5: 710-740, B6: 845-875 nm) spectral bands. For spectral bands all six spectral bands Gaussian function was considered as spectral response function. CRT model was run in forward mode with specific ground data as an input to simulate crop specific reflectance for MX-VNIR bands. The ground measured spectral signature from 400 to 2500 nm were also convoluted to six MX-VNIR bands. Model simulated and ground measured reflectance over different crops were compared.

### **4.4 Model inversion**

The various model input parameters listed in [Table 2](#) were divided into number of intervals within their ground observed lower and higher limits to cover whole dynamics of selected crop growth. The limits had been fixed on the basis of field measurements over various selected crop during 2014-16 and only leaf structure parameter was taken published data ([Nigam et al., 2014](#); [Fang et al., 2003](#); [Houborg and Boegh, 2008](#)). For agro-climatic regions, two distinct soil spectral libraries were generated from field observations which were used as an input for running the model over a selected zone. All the combination of different inputs according to their limits and intervals resulted into 1,500,00 input scenarios for all selected crops. The model was run in forward mode to generate simulated reflectances for four MX-VNIR spectral bands for all the scenarios for respective soil types of the region. Each set of simulated band reflectances generated through forward runs correspond to unique set of input parameters. Since present study aimed at retrieval of LAI, a look up table (LUT) was constituted from this simulated database of canopy reflectances and respective input parameters. The observed surface reflectances in LAI sensitive bands from MX-VNIR were then used to retrieve LAI through LUT inversion. An inversion technique based on least square approach was used to get the unique LAI for a given set of AVIRIS observed reflectances over agricultural crop. In this study LAI sensitive MX-VNIR bands were used for retrieval of LAI. In this study MX-VNIR data for LAI sensitive bands were generated using AVIRIS-NG (Air-borne Visible and Infrared Imaging Spectrometer-Next Generation) data. Through inversion of these observed bands from AVIRIS-NG convoluted to MX-VNIR, LAI over agricultural area were retrieved. A cost function (S) was used that represented the sum of square differences between convoluted AVIRIS pixel band reflectances and respective model simulated band reflectances. Minimum of the cost function was obtained using least square approach which gives

unique value of LAI for a given set of observed reflectances. This approach is similar to the variational method in which difference of error is minimized but differ in the sense of observation error covariance matrices. This may be the scope of future research under that variational approach (Barker et al., 2004) and can be used to retrieve the LAI from observed reflectance. In variational method, cost function, which is a function of total variance, is minimized. Here cost function is

$$S = (\rho_{b1simref} - \rho_{b1satref})^2 + (\rho_{b2simref} - \rho_{b2satref})^2 + (\rho_{b3simref} - \rho_{b3satref})^2 \quad (3a)$$

$$S = (\rho_{b1simref} - \rho_{b1satref})^2 + (\rho_{b2simref} - \rho_{b2satref})^2 + (\rho_{b3simref} - \rho_{b3satref})^2 + (\rho_{b4simref} - \rho_{b4satref})^2$$

(3b)

where  $\rho_{b1sim}$ ,  $\rho_{b2sim}$ ,  $\rho_{b3sim}$  and  $\rho_{b4sim}$  are simulated reflectances from b1, b2, b3 and b4 respectively and  $\rho_{b1satref}$ ,  $\rho_{b2satref}$ ,  $\rho_{b3satref}$  and  $\rho_{b4satref}$  are satellite observed reflectances in the respective bands. In this study equation 3a and 3b respectively used for three and four bands minimization. For minimum value of cost function (S), we differentiate S with respect to LAI as (Barker et al., 2004):

$$\frac{dS}{dLAI} = 0 \quad (4)$$

In this study different band combinations as per their sensitivity selected for retrieval of LAI.

Table 2. Input parameters to run *canopy radiative transfer* model

Model	Units	Symbol	Range
<b>PROSPECT</b>			
Leaf structure parameter	- - -	$N$	1-3
Chlorophyll a+b content	$\mu\text{g cm}^{-2}$	$C_{ab}$	20-80
Leaf equivalent water thickness	$C_m$	$C_w$	0.01-0.07
Leaf dry matter content	$\text{g cm}^{-2}$	$C_m$	0.001-0.025
Leaf size to crop height	- - -	$SI$	



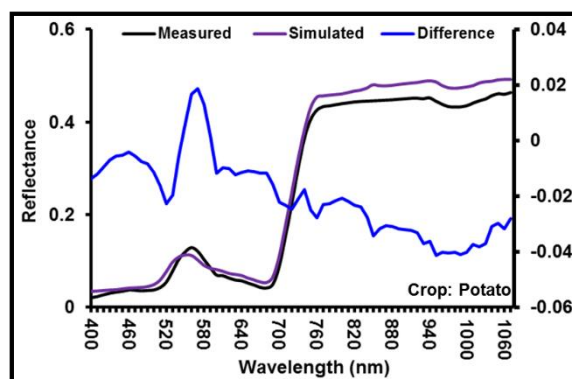
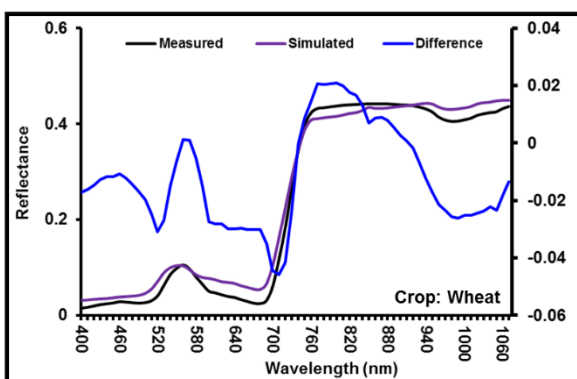
## SAIL

Leaf area index	---	LAI	0.5-6
Leaf inclination angle	---	LIA	5-60
Hot spot parameter	---	$S_L$	0.5//LAI
Horizontal visibility	m	VIS	5000

---

### 4.4 Calibration of model coefficient

The CRT model uses refractive index, leaf albedo, absorption coefficient for chlorophyll, water and dry matter to simulate reflectance for varying inputs. These coefficients were generated using lab based study over various vegetation leaves under varying leaf biochemical conditions. In model these coefficients were generated using pure spectral signature of different vegetation type specific to agriculture crop due to its variation in one dimension. In this study refractive index and coefficients for biomass has been calibrated using ground based input and spectral signature collected over different crop type at various crop stage. After calibrating with ground data in consideration with all selected crop for *rabi* and *Kharif*. Model was run in forwarded mode over various crop and compared with independent field dataset as shown in [Figure 3](#).



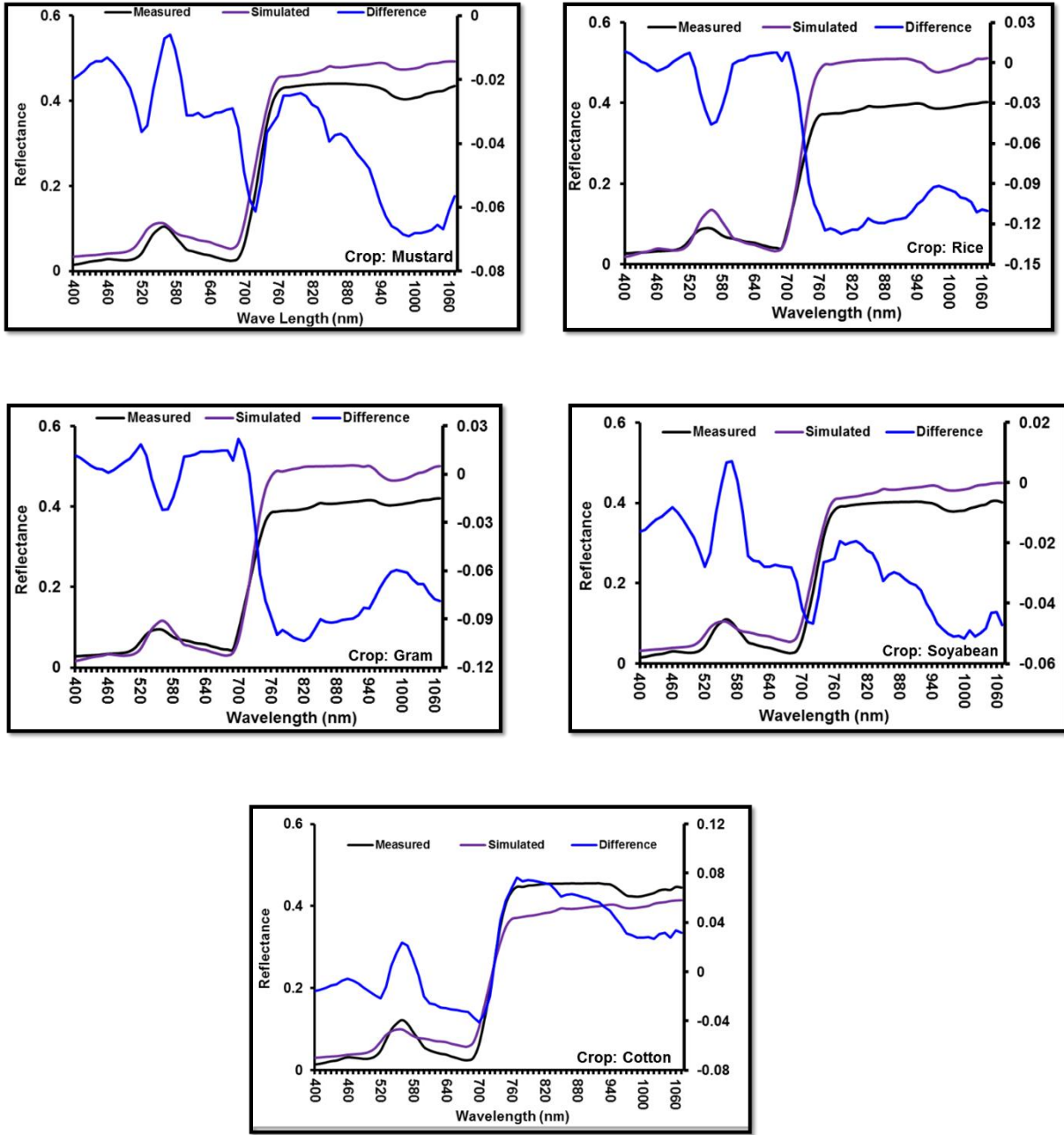


Figure 3. Comparison of measured and simulated spectral profile over different crops in selected agro-climatic zones

**5. Results**

**5.1 Sensitivity of Model for MX-VNIR bands**

After integration of all six bands and its spectral response characteristic into model one-dimensional sensitivity analysis was carried out for all intrinsic input parameters of model. The one dimensional sensitivity of model inputs for all six bands is shown in [Table 3](#). Here, typical mean values of parameters over observational sites at Kota were considered for sensitivity analysis. Parameters vary from its fixed value up to  $\pm 50\%$  at the interval of 10%. The simulated reflectances of six bands showed a different range of sensitivity towards LAI. The B1 (450-520 nm) showed coefficient of variation (CV) 2.2% and B2 band (520–590 nm) showed 6.6%. B3 (620-680 nm) showed high CV of 11.7% whereas B5 (710-740 nm) band again showed CV of 4.0% and both B4 bands (770-860 nm) and B6 (845-875 nm) again showed high CV of 16%. The B2 and B5 again showed low deviation between  $\pm 2\%$  deviation in reflectance while, B3 and B4 & b6 showed deviation between -12 to +10 and -18 to +20%, respectively. Leaf equivalent water thickness ( $C_w$ ) showed no deviation in all six bands due to its sensitivity to SWIR bands. The deviation of  $\pm 50\%$  in leaf internal structure parameter (N) showed a wide deviation in reflectances for all the six bands and it ranges from -21 to 25. The deviation in leaf chlorophyll (a + b) content ( $C_{ab}$ ) contributes to deviation of 80 to -28% for B1 and B2 band reflectances respectively and 60 to -15% for B3 and B5 spectral bands respectively. Both B4 & B5 bands showed no change in the reflectance with change in chlorophyll content as they are mostly affected by change in leaf thickness and water content. Leaf dry matter content ( $C_m$ ) showed a moderate deviation in all bands except in B4 & B5. These bands reflectances showed deviation between 21 to -16%. As  $C_m$  attributes to combination of all biochemical properties of leaf, it affects reflectances of all four bands. The shape of the absorption coefficient spectra slowly decreases between 450 nm and 800 nm for growing leaves. The absorption peak in the blue (420-480 nm) is probably caused by polyphenols (also called phenolic compounds), in particular flavonols ([Cerovic et al., 2002](#)). These compounds still exist in fresh foliage, but chlorophylls and carotenoids hide them. However, polyphenols are often correlated with leaf mean area (LMA), except for leaves on aging plants ([Meyer et al., 2006](#)). Hence, stronger absorption between 400 nm and 450 nm is also attributed to dry matter also. Deviation in leaf inclination angle (LIA) produces wide deviation in all the six bands of MX-VNIR. The range of percent deviation in all the bands is between 24 and -30. The one dimensional sensitivity analysis demonstrates the contribution of all leaf parameters towards six MX-VNIR band reflectances. The analysis showed that all six bands are sensitive to input model parameters except than leaf water thickness. Hence any change in input parameters excess leaf water content can be well captured through MX-VNIR band reflectances. Sensitivity revealed that four bands B2, B3, B4, B5 and B6 showed maximum sensitivity for LAI. Moreover, B4 and B6 both lie in NIR region only with different band width.

Table 3. One dimensional sensitivity analysis of CRT model inputs for six MX-VNIR bands

Variable	% deviation in variable value	% deviation in band reflectances					
		B1	B2	B3	B5	B4	B6
Leaf structure parameter (N)	-50 to +50	-8 to +25	-10 to +16	-5 to +20	-15 to +25	-21 to +19	-17 to +15
Chlorophyll a+b content( $C_{ab}$ )	-50 to +50	+35 to -14	+80 to -28	+58 to -11	+60 to -15	---	---
Leaf equivalent water thickness ( $C_w$ )	-50 to +50	--	--	--	--	--	--
Leaf dry matter content( $C_m$ )	-50 to +50	+0.9 to -0.6	+3 to -3	+0.7 to -0.3	+1 to -1.1	+21 to -15	+21 to -16
Leaf area index (LAI)	-50 to +50	+2 to -2	-0.4 to +4	+12 to -10	+4 to -4	-18 to +20	-19 to +22
Leaf inclination angle (LIA)	-50 to +50	+20 to -23	+24 to -30	+24 to -23	+21 to -24	+20 to -23	+20 to -23

## 5.2 Validation of retrieved LAI using MX-VNIR

In this study out of six MX-VNIR bands five showed sensitivity towards LAI at different capacities. Among all six bands B4 and B6 were lie in NIR region hence at time only one band was selected for retrieval of LAI. Total three combinations of bands (1) B2, B3, B4; (2) B2, B3, B6 and (3) B2, B3, B4, B5 were used to retrieve LAI using CRT model and AVIRIS convoluted bands over two sites at Kota region. The retrieved LAI using inversion of CRT model showed RMSE of 0.48 (18% deviation from measured mean) for B2B3B4 bands combination with ground measurements. RMSE will further increases to 1.0 (35%) and 1.6 (52%) respectively for B2B3B6 and B2B3B4B5

band combination. Fang et al. (2003) (RMSE = 1.0), Koetz et al. (2005) (RMSE = 0.5), Houborg et al. (2009) (RMSE = 0.65) over different vegetation types. Yi et al. (2008) particularly showed a RMSE = 0.7 over wheat crop using canopy radiative simulation model. The validation of retrieved LAI is shown in Figure 4.

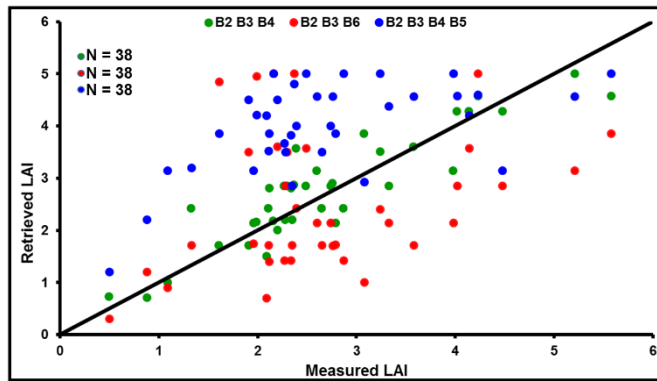


Figure 4. Validation of retrieved LAI from ground measurements

The histogram of agricultural LAI showed four (B2B3B4B5) bands always showed maximum value at higher range of LAI (Figure 5). Whereas, both three (B2B3B4 & B2B3B6) showed maximum value between 3 to 4 in both the sites.

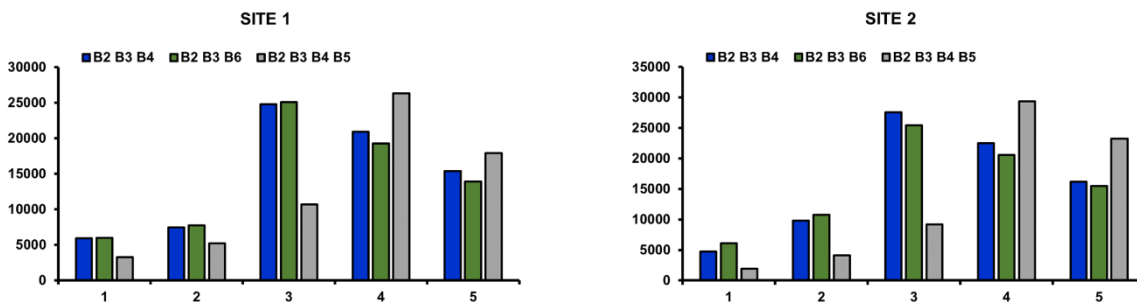


Figure 5. Histogram of LAI from retrieved LAI using various combination of MX-VNIR bands

The spatial distribution of retrieved LAI using different band combinations showed in Figure. From Figure 6 it was quite evident that four band combination always give higher LAI values and overestimation as compare to field measurements. In both the sites of Kota 60 percent agricultural area covered with wheat crop rest 25% comprises of crop such as mustard, chickpea, peas and coriander. The all bands able show low and high value of all crops. But band combination of B2B3B4B5 showed overestimation in all type of crops. The band combination of B2B3B4 showed

maximum heterogeneity at spatial scale as compare to other two. For the LAI value 1 to 2 first two band combination showed less difference on histogram but higher value it showed different behavior.

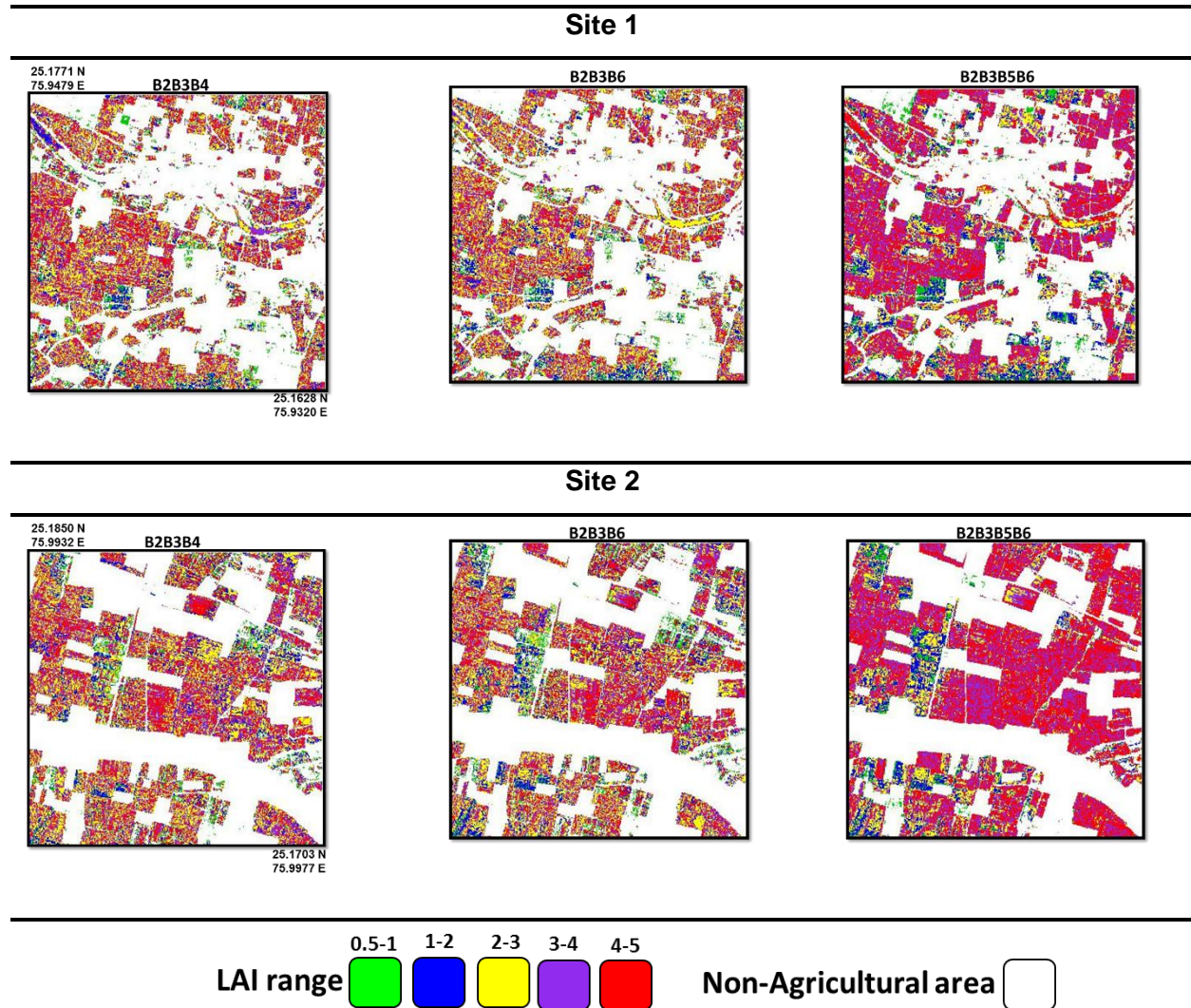


Figure 6. Spatial distribution of leaf area index (LAI) over agricultural area using three different set of MX-VNIR bands

## 6. Discussion

The above develop methodology is able to retrieve agricultural LAI over different crop type under agro-climatic conditions. However, its use for crops such as transplanted rice with standing water or crops under sub-mergence conditions is need to be further tested. Moreover, during high-wind

on clear days at the instance of satellite overpasses lead to alter observed satellite reflectances due to bending of leaves beyond the limit of leaf inclination angle considered for specific crop as an input for CRT model. It may result into different set of reflectances for LAI class. Prime advantage of simulation approach is the reduced independence on time and site-specific data but at the same time it requires sufficient number of appropriate spectrally and radiometrically accurate bands to get better results (Jacquemoud et al., 2009). As the reflectance data govern the accuracy of LAI estimation, inversions using coarse resolution data under the assumption of spatially homogeneous pixel will also introduce an error in the LAI estimation (Garrigues et al., 2006; Tian et al., 2002). The first contribution of the proposed algorithm is the dynamic update of LAI in agriculture season with identified three MX-VNIR bands. As a result, the retrieved LAI values could be used in crop and land surface model to update the crop growth monitoring and radiative fluxes. The method proposed here has taken advantage of routinely produced satellite data to provide LAI estimation. However, there still exist several limitations which need to be mentioned. The first limitation is related to the satellite data themselves, which are constrained by instabilities in observation such as calibration errors, atmospheric, cloud contamination, view-illumination geometry effects, and saturation of reflectance in dense canopies. Moreover, the quality flags accompanying the LAI and surface reflectance products do not infallibly identify their quality. In present study retrieved LAI is validated with limited number of sites in two agro-climatic zones. Consequently, this will not represent all agricultural systems of India. Moreover, the field-measured LAI values collected from existing research networks are each the mean value of several discrete sampled values. Certain errors associated with scale effect still exist. The ideal LAI data used to validate the retrieved LAI should be derived from high resolution imagery using ground based imager. This topic will be explored in future research.

## **7. Conclusions**

The pressing need for crop yield modeling and agricultural monitoring has led to a demand for high-quality, long-term consistent LAI products. However, currently available global LAI products may not meet the requirements from the viewpoint of accuracy, consistency and spatial resolution. Presently global various LAI products from CYCLOPES (1 km), ECOCLIMAP (1 km), GLOBCARBON (10 km) and MODIS (1 km) showed RMSE of 0.95, 1.56, 1.15 and 1.19 respectively over various vegetation types (Garrigues et al., 2008). Moreover, LAI gaps along with lag period for agricultural user due to various reasons also impose restrictions on the further application of data. The spatial resolution of GISAT (50 m) is adequate enough to ensure relatively accurate retrievals of LAI of agricultural crop at regional and high temporal scale. Presently in

India AWiFS has a 5-day revisit period which may cause loss of data due to persistent cloud or fog to retrieve LAI at all major crop growth stages. But GISAT daily data will provide more possibility to get clear sky data. The develop methodology will be used to generate LAI from future proposed Indian Geostationary Imaging Satellite (GISAT) mission.

### **Acknowledgments**

The authors would like to thank Director, Space Applications Centre, ISRO for his encouragement, motivation and support throughout this study. The authors would also like to thank Deputy Director, EPSA and Group Director, BPSG (SAC) for constant guidance. The authors also thank to GISAT: Science & Pre-launch preparatory Developments programme to provide opportunity for present study.

### **References**

- Allen, W.A., Gausman, H.W., Richardson, A.J., Thomas, J.R. (1969). Interaction of isotropic light with a compact plant leaf. *J. Opt. Soc. Am.* 59, 1376–1379.
- Anonymous, (2014). GISAT Payload Specifications Finalization Committee Report. SAC Report SAC/SEDA/GISAT-1/31-10-2014/06.
- Bacour, C., Baret, F., Béal, D., Weiss, M., & Pavageau, K. (2006). Neural network estimation of LAI, fAPAR, fCover and LAI × Cab, from top of canopy MERIS reflectance data: Principles and validation. *Remote Sens. Environ.*, 105, 313–325.
- Baret, F., & Guyot, G. (1991). Potentials and limits of vegetation indices for LAI and FAPAR assessment. *Remote Sens. Environ.*, 35, 161–173.
- Baret, F., Jacquemoud, S., Guyot, G., & Leprieur, C. (1992). Modeled analysis of the biophysical nature of spectral shifts and comparison with information content of broad bands. *Remote Sens. Environ.*, 41, 133–142.
- Barker, D.M., Huang, W., Guo, Y.R., Bourgeois, A.J., Xiao, Q.N. (2004). A three dimensional variational data assimilation system for MM5: implementation and initial results. *Mon. Weather Rev.* 132, 897–914.
- Bonan, G. B., Importance of leaf area index and forest type when estimating photosynthesis in boreal forests, *Remote Sens. Environ.*, 43, 303-314, 1993.



- Cerovic, Z. G., Ounis, A., Cartelat, A., Latouche, G., Goulas, Y., Meyer, S., et al. (2002). The use of chlorophyll fluorescence excitation spectra for the nondestructive in situ assessment of UV-absorbing compounds in leaves. *Plant Cell & Environment*, 25, 1663–1676.
- Chen, J.M., Black, T.A., 1992. Defining leaf area index for non-flat leaves. *Plant Cell Environ.* 15, 421–429.
- Fang, H., Liang, S., Kussk, A., (2003). Retrieving leaf area index using a genetic algorithm with a canopy radiative transfer model. *Remote Sens. Environ.* 85, 257–270.
- Garrigues, S., Allard, D., Baret, F., Weiss, M., (2006). Influence of landscape spatial heterogeneity on the non-linear estimation of leaf area index from moderate spatial resolution remote sensing data. *Remote Sens. Environ.* 105, 286–298. *J. of Geophys. Res.*, Vol. 113,, doi:10.1029/2007JG000635.
- Garrigues, S., Lacaze, R., Baret, F., Morisette, J. T., Weiss, M., Nickeson, J. E., Fernandes, R., Plummer, S., Shabanov, N.V., Myneni, R.B., Knyazikhin, Y., Yang, W. (2008). Validation and intercomparison of global Leaf Area Index products derived from remote sensing data.
- Houborg, R., Anderson, M., Daughtry, C., 2009. Utility of an image-based canopy reflectance modeling tool for remote estimation of LAI and leaf chlorophyll content at the field scale. *Remote Sens. Environ.* 113, 259–274.
- Houborg, R., Boegh, E., (2008). Mapping leaf chlorophyll and leaf area index using inverse and forward canopy reflectance modeling and SPOT reflectance data. *Remote Sens. Environ.* 112, 186–202.
- Jacquemoud, S., Baret, F., 1990. PROSPECT: a model of leaf optical properties spectra. *Remote Sens. Environ.* 34, 75–91.
- Jacquemoud, S., Verhoef, W., Baret, F., Bacour, C., Zarco-Tejada, P.J., Asner, G.P., Franc, O. C., Ustin, S.L., 2009. PROSPECT + SAIL models: a review of use for vegetation characterization. *Remote Sens. Environ.* 113, S56–S66.
- Koetz, B., Baret, F., Poilve, H., Hill, J., 2005. Use of coupled canopy structure dynamics and radiative transfer model to estimate biophysical canopy characteristics. *Remote Sens. Environ.* 95, 115–124.

- Liu, Q., Liang, S., Xiao, Z. and Fang, H. (2014). Retrieval of leaf area index using temporal, spectral, and angular information from multiple satellite data. *Remote Sens. Environ.*, 145, 25-37.
- Marie, G., Marsden, C., Verhoef, W., Ponzoni, F., Seen, D., Bégué, A., Stape, J., Nouvellon, Y. (2011). Leaf area index estimation with MODIS reflectance time series and model inversion during full rotations of Eucalyptus plantations. *Remote Sens. Environ.*, 115, 586-599.
- Meyer, S., Cerovic, Z. G., Goulas, Y., Montpied, P., Demotes-Mainard, S., Bidet, L. P. R., et al. (2006). Relationships between optically assessed polyphenols and chlorophyll concentrations, and leaf mass per area ratio in woody plants: A signature of the carbon–nitrogen balance within leaves? *Plant, Cell & Environment*, 29, 1338–1348.
- Nigam, R., Bhattacharya, B. K., Vyas, S., Oza, M.P. (2014). Retrieval of wheat leaf area index from AWiFS multispectral data using canopy radiative transfer simulation. *Int. J. App. Earth Obs. and Geoinform.* 32, 173–185.
- Propastin, P. and Erasim, S. (2010). A physically based approach to model LAI from MODIS 250 m data in a tropical region. *Int. J. App. Earth Obs. and Geoinform.* 12, 47–59.
- Running, S.W., Thornton, P.E., Nemani, R., 2000. Global terrestrial gross and net primary productivity from the earth observing system. In: Sala, O.E., Jackson, R.B., Mooney, H.A., Howarth, R.W. (Eds.), *methods in Ecosystem Science*. Springer–Verlag, New York, pp. 44–57.
- Schaepman-Strub, G., Schaepman, M.E., Painter, T.H., Dangel, S., Martonchik, J.V., 2006. Reflectance quantities in optical remote sensing – definitions and case studies. *Remote Sens. Environ.* 103, 27–42.
- Seller, P.J., Dickinson, R.E., Randall, D.A., Betts, A.K., Hall, F.G., Berry, J.A., Collatz, G.J., Denning, A.S., Mooney, H.A., Nobre, C.A., Sato, N., Field, C.B., Henderson-Sellers, A., 1997. Modeling the exchanges of energy, water, carbon between continents and the atmosphere. *Science* 275, 502–509.
- Shabanov, N. V., Huang, D., Yang, W., Tan, B., Knyazikhin, Y., Myneni, R. B., et al. (2005). Analysis and optimization of the MODIS leaf area index algorithm retrievals over broadleaf forests. *IEEE Transactions on Geoscience and Remote Sensing*, 43, 1855–1865.

- Tian, J., & Chen, D. (2010). A semi-empirical model for predicting hourly ground-level fine particulate matter (PM<sub>2.5</sub>) concentration in southern Ontario from satellite remote sensing and ground-based meteorological measurements. *Remote Sensing of Environment*, 114, 221–229.
- Tian, Y., Wang, Y., Zhang, Y., Knyazikhina, Y., Bogaert, J., Myneni, R.B., (2002). Radiative transfer based scaling of LAI/FPAR retrievals from reflectance data of different resolutions. *Remote Sens. Environ.* 84, 143–159.
- Verhoef, W., 1984. Light scattering by leaf layers with application to canopy reflectance modeling: the SAIL model. *Remote Sens. Environ.* 16, 125–141.
- Verhoef, W., Bach, H., 2003. Simulation of hyperspectral and directional radiance images using coupled biophysical and atmosphere radiative transfer model. *Remote Sens. Environ.* 87, 23–41.
- Walthalla, C., Dulaneya, W., Anderson, M., Norman, J., Fang, H., & Liang, S. (2004). A comparison of empirical and neural network approaches for estimating corn and soybean leaf area index from Landsat ETM + imagery. *Remote Sens. Environ.*, 92, 465–474.
- Xiao, Z., Liang, S., Wang, J., Chen, P., Yin, X., Zhang, L., et al. (2013). Use of general regression neural networks for generating the GLASS leaf area index product from time series MODIS surface reflectance. *IEEE Transactions on Geoscience and Remote Sensing*, 1–15.
- Yi, Y., Yang, D., Huang, J., Chen, D., 2008. Evaluation of MODIS surface reflectance products for wheat leaf area index (LAI) retrieval. *ISPRS J. Photo Remote Sens.* 63, 661–677.